

# <sup>1</sup> multimodars: A Rust-powered toolkit for <sup>2</sup> multi-modality cardiac image fusion and registration

<sup>3</sup> **Anselm W. Stark**  <sup>1,2</sup>¶, **Marc Ilic**  <sup>1,2</sup>, **Ali Mokhtari**  <sup>1,2</sup>, **Pooya**  
<sup>4</sup> **Mohammadi Kazaj**  <sup>1,2</sup>, **Christoph Gräni**  <sup>1</sup>, and **Isaac Shiri**  <sup>1</sup>

<sup>5</sup> 1 Department of Cardiology, Inselspital, Bern University Hospital, University of Bern, Switzerland 2

<sup>6</sup> Graduate School for Cellular and Biomedical Sciences, University of Bern, Bern, Switzerland ¶

<sup>7</sup> Corresponding author

DOI: [10.xxxxxx/draft](https://doi.org/10.xxxxxx/draft)

## Software

- [Review](#) ↗
- [Repository](#) ↗
- [Archive](#) ↗

Editor: **Erick Martins Ratamero** 

## Reviewers:

- [@jonaspleyer](#)
- [@richardkoehler](#)
- [@crnh](#)

Submitted: 28 August 2025

Published: unpublished

## License

Authors of papers retain copyright<sup>22</sup> and release the work under a Creative Commons Attribution 4.0 International License ([CC BY 4.0](#))<sup>23</sup>.

## <sup>8</sup> Summary

<sup>9</sup> Coronary artery anomalies (CAAs) and coronary artery disease (CAD) require precise  
<sup>10</sup> morphological and functional assessment for diagnosis and treatment planning. Cardiac  
<sup>11</sup> computed tomography angiography (CCTA) provides a comprehensive 3D coronary anatomy  
<sup>12</sup> but lacks the sub-millimeter resolution and dynamic tissue detail available from intravascular  
<sup>13</sup> imaging, such as intravascular ultrasound (IVUS) and optical coherence tomography (OCT).

<sup>14</sup> The multimodars package is a general-purpose toolkit that registers high-resolution  
<sup>15</sup> intravascular pullbacks to CCTA-derived centerlines, producing locally enhanced fusion 3D  
<sup>16</sup> vessel representations. Developed initially to quantify dynamic lumen changes in CAAs,  
<sup>17</sup> the toolkit produces high-fidelity models suitable for visualization, geometric analysis,  
<sup>18</sup> and patient-specific modelling. It implements four alignment paradigms (full, double-pair,  
<sup>19</sup> single-pair, single) to compare pullbacks acquired under different haemodynamic states (e.g.,  
<sup>20</sup> rest vs. pharmacologic stress) or at different clinical timepoints (e.g., pre- vs. post-stenting).  
<sup>21</sup> Multimodars targets deterministic, reproducible multimodal fusion for both specialized CAA  
<sup>22</sup> research and general CAD applications ([Anselm Walter Stark et al., 2025](#)).

## <sup>23</sup> Statement of Need

<sup>24</sup> Building reliable 3D coronary models requires combining complementary imaging modalities.  
<sup>25</sup> Intravascular imaging offers exceptional local resolution but lacks whole-vessel context and 3D  
<sup>26</sup> orientation. CCTA provides the global 3D geometry but suffers from limited spatial resolution  
<sup>27</sup> and artifacts like blooming. Multimodars fills a critical gap for researchers in **cardiac imaging**,  
<sup>28</sup> **interventional cardiology**, and **biomedical engineering** who require high-fidelity lumen models  
<sup>29</sup> for:

- <sup>30</sup> ▪ Automated quantification of vessel deformation under stress.
- <sup>31</sup> ▪ Computational Fluid Dynamics (CFD) and Fluid-Structure Interaction (FSI) simulations.
- <sup>32</sup> ▪ Digital twin solutions.

<sup>33</sup> The package accepts CSV and NumPy inputs, including data formats produced by the **AIIVUS-**  
<sup>34</sup> **CAA** software ([Anselm W. Stark et al., 2025](#)), providing a standardized pipeline from raw  
<sup>35</sup> image segmentation to final 3D fusion.

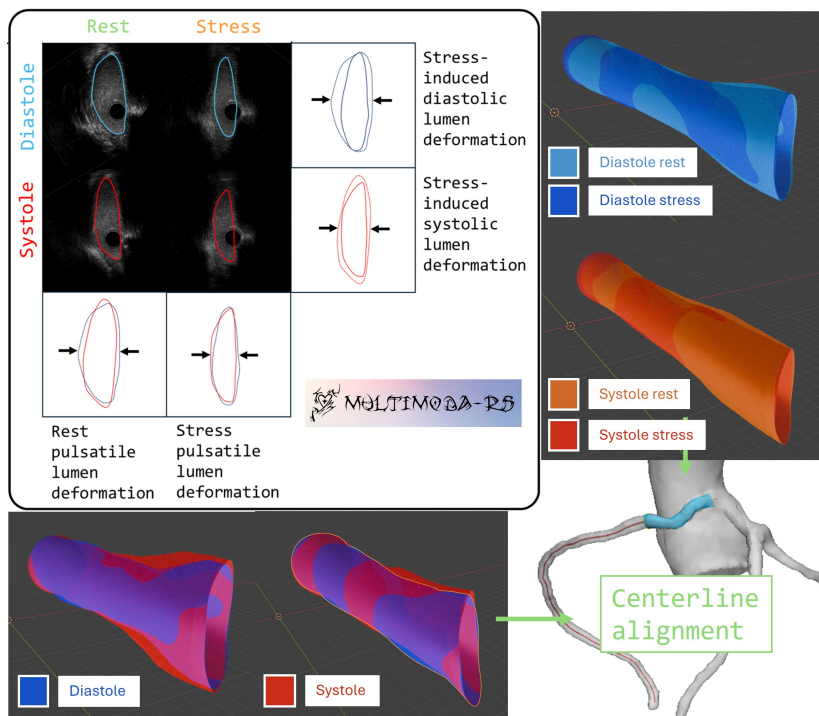


**Figure 1:** Figure 1: Illustration of multimodars processing modes and their clinical use. The ‘full’ mode returns four geometry pairs to analyze rest and stress haemodynamics (rest pulsatile deformation; stress pulsatile deformation; stress-induced diastolic deformation; stress-induced systolic deformation). The ‘double-pair’ mode returns pulsatile deformation in rest and stress. ‘Single-pair’ compares any two states (e.g., pre-/post-stent). ‘Single’ aligns frames within one pullback.

## 36 State of the Field

37 Prior research has established the clinical value of CCTA/intravascular fusion (Boogers et al.,  
 38 2012; Bourantas et al., 2013; Giessen et al., 2010; Ilic et al., 2025; Wu et al., 2020), but  
 39 several barriers remain: 1. **Proprietary Constraints**: Most existing fusion solutions are tied  
 40 to proprietary vendor hardware or closed-source commercial workstations, limiting academic  
 41 transparency. 2. **Multi-state Gap**: No existing open-source toolkit is specifically tailored  
 42 for **multi-state** analysis (comparing rest vs. stress or pre- vs. post-intervention states) while  
 43 maintaining a deterministic alignment across pullbacks.

## 44 Build vs. Contribute Justification

45 While packages like trimesh or SimpleITK provide general mesh and registration utilities, they  
 46 do not offer the domain-specific coronary alignment logic (e.g., cumulative rotation propagation  
 47 to preserve vessel torsion) required for intravascular imaging. Multimodars was built as a  
 48 standalone toolkit because existing registration libraries lack the specific coordinate mapping  
 49 and multiscale search algorithms optimized for curvilinear cardiac centerlines.

## 50 Software Design

51 Multimodars is built as a maturin project, wrapping a high-performance Rust core with a  
 52 Python interface.

## 53 Architectural Choices and Trade-offs

- 54 We chose **Rust** for the core backend to leverage its memory safety and hierarchical data  
 55 parallelism (via the Rayon crate). This allows the toolkit to handle the significant computational  
 56 load of multiscale angular searches across hundreds of image frames without the performance  
 57 limitations found in pure Python implementations.
- 58 The data model uses a compact typed structure (PyContourPoint, PyContour, PyGeometry)  
 59 that maps losslessly to (N,4) NumPy arrays (frame\_id, x, y, z). This choice balances the  
 60 performance of low-level data structures with the usability of the Python data science ecosystem.

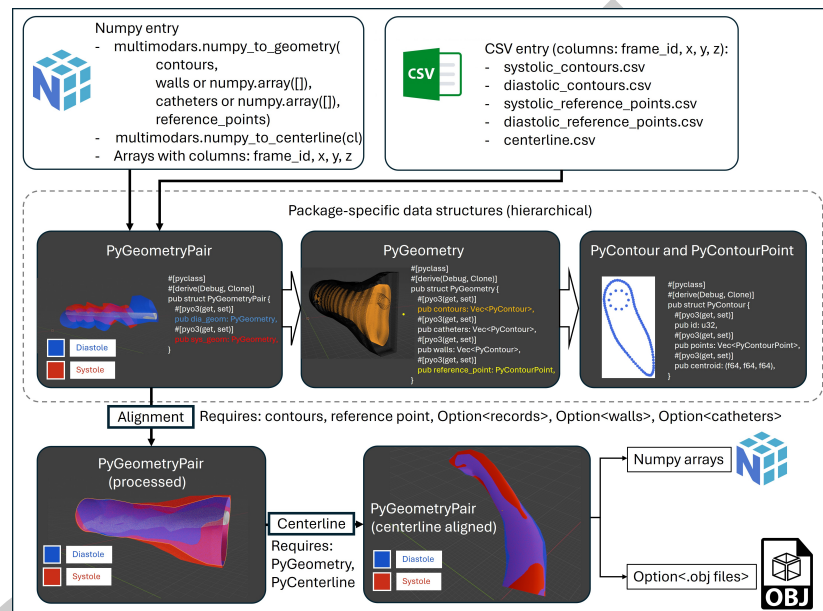


Figure 2: Internal data model and (N,4) NumPy mapping used by `multimodars` (`frame_id`, `x`, `y`, `z`).

## 61 Algorithms

62 Alignment is a two-stage pipeline producing spatially and rotationally consistent mappings both  
 63 within pullbacks (intra-pullback) and between pullbacks (inter-pullback). It further aligns 3D  
 64 models with a CCTA derived centerline and adjusts the CCTA mesh to match the dimensions  
 65 of the intravascular 3D model.

- 66 **Intra-pullback:** The proximal frame is the rotational reference. Sequentially, each  
 67 proximal→distal neighbour is aligned by centroid translation and a rotation search  
 68 minimizing a point-set distance derived from directed Hausdorff distances. Rotation  
 69 employs a multiscale angular search (coarse → fine, e.g.,  $1^\circ \rightarrow 0.1^\circ \rightarrow 0.01^\circ$ ) with  
 70 cumulative rotation propagation to preserve vessel torsion (See [Figure 4](#)). Naive brute-  
 71 force complexity scales as  $O(n \times \frac{R}{S} \times m^2)$  ( $n$  = frames,  $m$  = points per contour,  $R$   
 72 = angular range,  $S$  = step size). By fixing contour size (downsampling) and reducing  
 73 the angular search via multiscale refinement, the pipeline attains effective complexity  
 74  $O(n \times (R + c) \times m^2)$  for small  $S$ , making runtime less sensitive to step granularity while  
 75 preserving alignment accuracy.
- 76 **Inter-pullback and CCTA fusion:** Inter-pullback alignment harmonizes distal centroids,  
 77 averages slice spacing to align z-coordinates, and applies a rigid rotation to minimize mean  
 78 directed distances across corresponding frames; ellipticity-weighted similarity prioritizes  
 79 non-round stenotic slices.

- 80     ▪ **CCTA-Centerline alignment:** The multimodars package implements a three-point
- 81       (aortic-, cranial- and caudal direction) anatomical registration and a manual alignment
- 82       mode. It additionally utilizes Hausdorff distances to CCTA mesh points for ambiguous
- 83       anatomies: centerlines are resampled to contour spacing, centroids are translated to
- 84       matched points, normals are aligned by cross-product computations, and an optional
- 85       interpolated UV-mapped mesh is produced for visualization and downstream modeling.
- 86     ▪ **CCTA-labeling:** For normal coronary anatomy, CCTA mesh points are labeled using a
- 87       rolling-sphere sweep along the coronary centerline. For CAAs, where the vessel may run
- 88       very close to or within the aortic wall, this is followed by an occlusion-based cleanup:
- 89       rays are cast from the aortic centerline toward the coronary centerline; ray-triangle
- 90       intersections identify occluding aortic wall regions, and mesh points close to these
- 91       surfaces are removed. This yields a deterministic and anatomically consistent coronary
- 92       lumen representation.
- 93     ▪ **CCTA-border adjustments:** Given the higher resolution of intravascular imaging, the
- 94       aligned intravascular anatomy is treated as the anatomical ground truth. CCTA
- 95       dimensions are adjusted to fit the proximal and distal ends of the vessel. For CAAs, the
- 96       aorta is additionally adjusted to match the measured intramural wall.

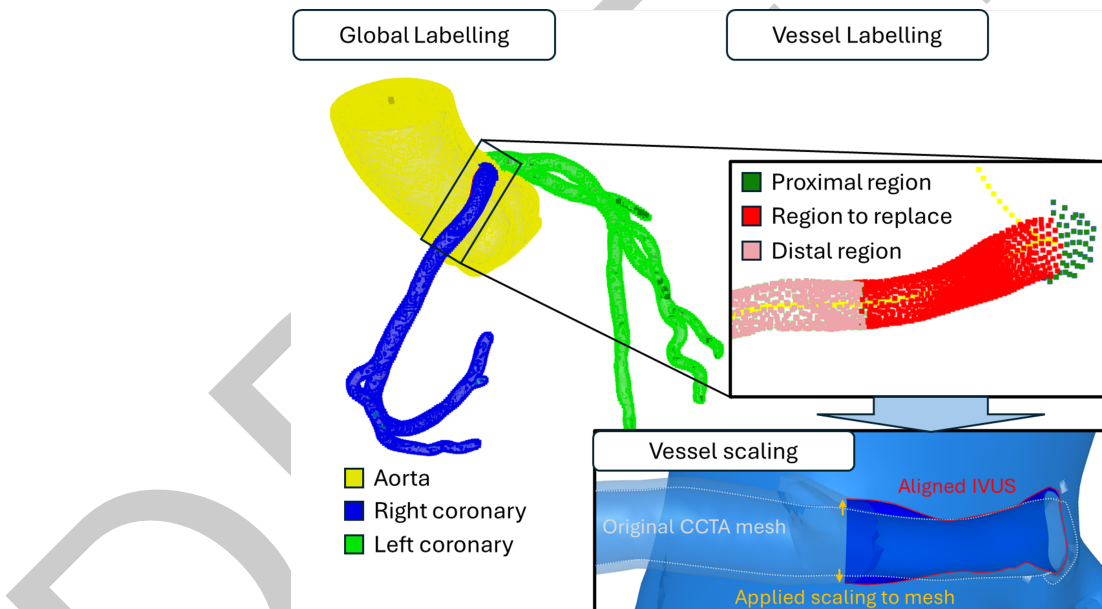


**Figure 3:** Figure 3: Top left shows the initial labeling of the coronary arteries and aorta based on centerlines. In a second step the regions to be replaced are identified based on the aligned 3D intravascular model. In a last step the CCT proximal and distal borders can be adjusted to best match intravascular borders.

## 97     Performance and parallelisation

98     Rust (Rayon) provides hierarchical data parallelism and SIMD-enabled coordinate transforms.  
 99     Point rotations and nearest-neighbour searches parallelize across cores; independent pullbacks  
 100    and frames are processed concurrently when dependencies allow. Typical production workflows  
 101    downsample contours to 200–500 points/frame to balance sub-pixel accuracy and compute.  
 102    Empirical performance on a 16-core CPU: an OCT pullback with 280 frames and a rotation  
 103    search range of  $\pm 3^\circ$  (final accuracy  $0.01^\circ$ ) saw alignment time reduced from  $150\text{s}$  to  $18\text{s}$   
 104    with the optimized multiscale search.

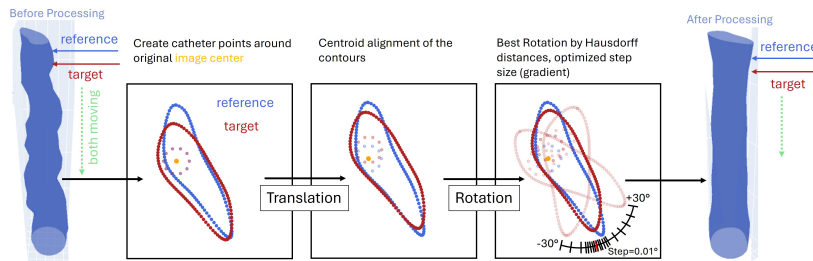


**Figure 4:** Figure 4: Multiscale intra-pullback alignment workflow (coarse-to-fine angular search and centroid propagation).

## 105 Implementation, reproducibility and usage

106 The core is implemented in Rust and exposed to Python via PyO3; packaging uses maturin  
 107 and the package is available on PyPI. The NumPy-centric API maps directly to (N,4) arrays;  
 108 the project includes example notebooks, sample data (including AIVUS-CAA (Anselm W.  
 109 Stark et al., 2025)) and CI tests. Documentation and tutorials are hosted on ReadTheDocs  
 110 ([ReadTheDocs](#)).

## 111 Research impact statement

112 Multimodars was motivated by the need to quantify dynamic lumen deformation in CAAs, where  
 113 rest/stress and pulsatile comparisons are diagnostically critical. Deterministic, high-resolution  
 114 fusion enables quantitative assessment of stress-induced deformation and supports patient-  
 115 specific haemodynamic modeling. These methods also support longitudinal CAD analyses (e.g.,  
 116 pre-/post-stent). In a case report accepted in JACC: Case Reports, we successfully implemented  
 117 this fusion approach to unveil a distinct compression pattern not visible in IVUS or CCTA  
 118 alone. We hope to foster a research community that leverages multimodars to standardize  
 119 multimodal coronary fusion and accelerate the development of personalized interventional or  
 120 computational strategies.

## 121 AI usage disclosure

122 No generative AI was used for architectural design or core algorithms. Generative AI was used  
 123 for creating documentation docstrings, bug fixing, and minor inline code changes. For this  
 124 manuscript generative AI was only used for grammatical changes.

## 125 Acknowledgements

126 None

## 127 References

- 128 Boogers, M. J., Broersen, A., Van Velzen, J. E., De Graaf, F. R., El-Naggar, H. M.,  
 129 Kitslaar, P. H., Dijkstra, J., Delgado, V., Boersma, E., Roos, A. de, & others. (2012).  
 130 Automated quantification of coronary plaque with computed tomography: Comparison  
 131 with intravascular ultrasound using a dedicated registration algorithm for fusion-based  
 132 quantification. *European Heart Journal*, 33(8), 1007–1016.
- 133 Bourantas, C. V., Papafakis, M. I., Athanasiou, L., Kalatzis, F. G., Naka, K. K., Siogkas,  
 134 P. K., Takahashi, S., Saito, S., Fotiadis, D. I., Feldman, C. L., & others. (2013). A

- 135 new methodology for accurate 3-dimensional coronary artery reconstruction using routine  
136 intravascular ultrasound and angiographic data: Implications for widespread assessment of  
137 endothelial shear stress in humans. *EuroIntervention*, 9(5), 582–593. <https://doi.org/10.4244/EIJV9I5A94>
- 139 Giessen, A. G. van der, Schaap, M., Gijsen, F. J., Groen, H. C., Walsum, T. van, Mollet, N. R.,  
140 Dijkstra, J., Vosse, F. N. van de, Niessen, W. J., Feyter, P. J. de, & others. (2010). 3D  
141 fusion of intravascular ultrasound and coronary computed tomography for in-vivo wall shear  
142 stress analysis: A feasibility study. *The International Journal of Cardiovascular Imaging*,  
143 26(7), 781–796. <https://doi.org/10.1007/s10554-009-9546-y>
- 144 Ilic, M., Häner, J., Lehmann, J., Stark, A. W., Illi, J., Gräni, C., Bentele, M., Baumann-  
145 Zumstein, P., Busch, J., & Haeberlin, A. (2025). A comprehensive workflow for CCTA  
146 and OCT data fusion with 3D printing validation: Advancing patient-specific testing  
147 environments for percutaneous coronary intervention devices. *BioMedical Engineering  
148 OnLine*.
- 149 Stark, Anselm Walter, Bigler, M. R., Räber, L., & Gräni, C. (2025). True pulsatile  
150 lumen visualization in coronary artery anomalies using controlled transducer  
151 pullback and automated IVUS segmentation. *Case Reports*, 30(22), 104741.  
152 <https://doi.org/10.1016/j.jaccas.2025.104741>
- 153 Stark, Anselm W., Kazaj, P. M., Balzer, S., Ilic, M., Bergamin, M., Kakizaki, R., Giannopoulos,  
154 A., Haeberlin, A., Räber, L., Shiri, I., & others. (2025). Automated intravascular ultrasound  
155 image processing and quantification of coronary artery anomalies: The AIVUS-CAA software.  
156 *Computer Methods and Programs in Biomedicine*, 109065.
- 157 Wu, W., Samant, S., De Zwart, G., Zhao, S., Khan, B., Ahmad, M., Bologna, M., Watanabe,  
158 Y., Murasato, Y., Burzotta, F., & others. (2020). 3D reconstruction of coronary artery  
159 bifurcations from coronary angiography and optical coherence tomography: Feasibility,  
160 validation, and reproducibility. *Scientific Reports*, 10(1), 18049. <https://doi.org/10.1038/s41598-020-74264-w>